Green synthesis of graphene-coated glass as novel reactive material for remediation of fluoride-contaminated groundwater

Ziad T. Abd Ali

Department of Environmental Engineering, College of Engineering-University of Baghdad/Iraq, email: z.teach2000@yahoo.com

ABSTRACT

The intent of this study was to elucidate a novel green method using low-grade Iraqi dates and glass waste granules to synthesize graphene-coated glass (GCG). This is a novel, economical, and effective reactive material that is very useful in permeable reactive barrier methodology for the remediation of fluoride-contaminated groundwater. The sorption process is controlled by factors such as the contact time, agitation speed, pH, and GCG dosage, which were investigated during batch processing. Two isotherm models (Langmuir and Freundlich) were used to explain the sorption data, while the continuous experimental results were fitted to the Bohart–Adams, Thomas–Bed Depth Service Time, and Clark breakthrough curve models. In the set of continuous experiments, the GCG-barrier performance was monitored, employing the concentrations of the effluent fluoride using different thicknesses of the barrier, inlet initial fluoride concentrations, and rates of flow.

Keywords: Graphene-coated glass; Fluoride; Sorption; Permeable reactive barrier; Transport

1. Introduction

Water, both surface and ground sources, is the worthy natural resource that sustains all living organisms on earth. Sadly, during recent decades, a reduction in water quality is clearly evident. This has been triggered because of human practices like widespread urban development, the alarming explosion of population, increase in industries, and heedless use of natural resources, especially water. Water gets polluted by several means, such as the indiscriminate disposal of toxic waste materials from industries, as well as the dumping of non-treated sanitary waste and runoffs from agricultural practices [1–3].

Besides anthropogenic influences, groundwater pollution takes place through natural means. When fluoride-rich rocks and other types of minerals like fluorspar, cryolite, and fluorapatite get dissolved in both ground and surface water, they become the principal sources of natural contamination, releasing the F⁻ in the soil [4,5]. Further, the fluoride chemical industry, and those involved in the processing of the semiconductors and metals, the production of fertilizer and glass manufacture, release runoffs which also add to the water contamination [6].

According to the World Health Organization (WHO) classification, F⁻ remains among the principal contaminants of our water resources; therefore, it has been suggested to set the limit at as low as 1.5 mg/L for F⁻ in drinking water as the maximum permissible level [7]. When the F⁻ concentration exceeds this limit, it is seen to cause damage to human health, in terms of fluorosis, arthritis and brittle bones. Further, long-period exposure to conditions of excessive F⁻ can lead to major health problems such as causes of immunological and birth defects and even cancer [8]. From a global perspective, in a little over 20 countries, including China, Africa, Sri Lanka, and even India the effects of endemic fluorosis are evident. In India, around many states have been declared fluoride endemic, with the health of nearly 1 million people being affected [9]. Therefore, the toxicity induced by excessive F⁻ in the water makes it crucial to lower this F⁻ level, until it achieves the prescribed concentration. Over the recent

years, the use of many technologies and methods such as adsorption, ion-exchange, precipitation and electro-dialysis for F⁻ removal from the water sources have been in use [10].

The ex-situ pump-and-treat system is the commonest groundwater remediation method in use. This system draws the groundwater up to the surface and then treats it via different processes like adsorption. The treated water is then returned to the underground or discharged into a storm water drain. While this method is neither easy nor economical, it is frequently quite ineffective in removing sufficient quantities of the contaminant to raise the quality of the groundwater to the agreeable standards for drinking water, within reasonable time periods [11]. Therefore, the technology of permeable reactive barriers (PRBs) emerged as a good alternative for the remediation of groundwater polluted with a variety of contaminants [12]. Clearly, this was better than the pump-and-treat method, and showed higher potential to contain the contaminant spread. Further, PRB is very popular globally and applied extensively because its removal efficiency is high, maintenance and economic investment are low, durability (about 10–20 y) is good, and it is environmentally safe [13]. However, in the permeable barriers, it is mandatory to use an inexpensive, subsurface environment-compatible reactive material, with no undesirable reactions and no possibility of being a source of contamination [14].

Although many choices of several naturally present and economical reactive materials amenable to the PRB are available, there continues to be a search to design an absorbent with high efficiency, economic affordability and strong removal abilities [15]. Much research has been done using cheap and beneficial substances, such as the reactive material in PRB technology namely, activated carbon produced using Iraqi date pits or seeds, olive seeds, graphene-coated sand, granular dead anaerobic sludge, and concrete demolition waste [2,12,14,16–20].

This work attempts to accomplish the green synthesis of graphene-coated glass (GCG) as a novel, successful, sustainable, and low-cost reactive material for the remediation of fluoride-contaminated groundwater using PRB technology. Although many research papers on graphene-coated materials are available [21–24], the originality of this work, which makes it different from the others, is the use of low-grade Iraqi dates. These dates principally containing carbohydrates (sucrose and fructose) are a high carbon source, very affordable, and sustainable. They are a good source of carbon and their complete non-toxicity to both humans and the environment, (inducing neither side effects nor allergies) makes them attractive to use [14]. Further, based on the significant environmental principles such as sustainable, reusable, and environmental preservation of waste, the granules of crushed glass waste were used as the core material for the coating process by graphene.

In light of the discussion above, this study aims at exploring the potential application of GCG as a novel reactive material in the remediation of fluoride-contaminated groundwater via PRB technology, through batch and continuous experiments. This was accomplished by (a) synthesizing a novel graphenized glass called GCG as a novel and low-cost reactive material, (b) determining the characteristics of the new reactive material (GCG) through several

tests (c) studying the effect of several parameters such as contact time, agitation speed, pH, and GCG-dosage on the fluoride removal efficiency in batch experiments, and (d) for continuous study, characterizing experimentally the one-dimensional equilibrium fluoride transport through the GCG fixed-bed column, and theoretically employing the breakthrough curve models mentioned earlier.

2. Materials and methods

2.1. Materials

The GCG to be used as a reactive media for PRB was synthesized using low-quality Iraqi dates as low-cost carbon source and granules of crushed glass waste as core material for the graphene-coating process. The other chemicals used included an activating reagent (sulfuric acid of high-grade purity) and an adsorbate (sodium fluoride).

2.2. Preparation of GCG

The GCG was prepared by adopting the following three steps: first, the glass waste was collected, washed, crushed, and sieved into granules, 1–0.6 mm in diameter, and low-quality Iraqi dates were used as the natural, sustainable and low-cost carbon source. The date flesh (minus the date seeds) was then weighed, subjected to 20 min of boiling time in sufficient water. It was then blended, and this slurry was filtrated using a cloth filter with hand press. This date juice extract was then collected and after subjecting it to 30 min of centrifugation at 5,000 rpm, the clear filtrate was then passed through a rotary evaporator. The concentration was performed at 70°C under vacuum conditions. Next, this date juice was collected, and the requisite quantity of glass granules was added, after stirring it was placed in a hot air oven set at 90°C, till the juice of date consolidate on the surface of the glass granules. In the second stage, the mixture of date juice and glass was burned for 3 h in a furnace at 750°C under N₂ gas atmosphere to prevent oxidation. When the fusion point of the consolidate date juice was reached, at 185°C, the sample changed in color and became dark brown. The carbon material was thus obtained by the conversion of the sucrose and fructose molecules in the date juice. The third and final step implicated the activation process which was done by the addition of sulfuric acid to clean the surface from ashes. Then, the GCG was filtered, washed, and dried at 105°C for a 2 h time period [14]. The final product, a black material (GCG), was cooled and then sieved with pore size of 1–0.6 mm in diameter. The GCG showed solid density of 2.92 g/cm³, bulk density of 1.61 g/cm³, and porosity of 0.45.

2.3. Preparation of fluoride solution

First, the simulated fluoride-contaminated groundwater of 10 mg/L concentration was fabricated by dissolving the necessary amount of NaF in distilled water. The remaining concentration of F⁻ in the remediated aqueous solutions was ascertained using the combined ion-selective electrode (InoLab pH/ION/Cond 750, WTW). To get even higher accuracy, the fluoride concentrations

were triple-checked using ion chromatography (Model: Metrohm Swiss 881 Compact IC 2008).

2.4. Characterization of GCG

Prior to utilizing, the GCG characterization was done by performing the tests listed below:

2.4.1. Fourier-transform infrared spectroscopy

The Fourier-transform infrared spectroscopy (FTIR) spectra of the prepared reactive media (GCG) were recorded using the 800 Series Shimadzu FTIR Spectrophotometer (Japan). The GCG was mixed with KBr to be used as the reference, and the spectral analyses of these samples were done. The spectra were identified to be in the 4,000–400 cm⁻¹ range.

2.4.2. Scanning electron microscope/energy-dispersive X-ray spectroscopy analysis

Using a scanning electron microscope and an energy-dispersive X-ray spectroscopy (SEM/EDX, TESCAN, VEGA III, Czech Republic), the surface morphology, and the constituent analysis of the glass granules and GCG were studied.

2.4.3. Specific surface area

The method of nitrogen adsorption was applied to confirm the GCG surface area via the Quantachrome NovaWin software for data acquisition and reduction for the NOVA Instruments at 77.3 K.

2.5. Batch experiments

The influences exerted by the operating conditions on the optimal efficiency of fluoride removal were investigated via the batch experiments. These conditions extended to the contact time, agitation speed, solution pH at the beginning of the experiment, and the GCG dosage. The batch experiments involved four steps, maintaining the primary F⁻ concentration (10 mg/L) and GCG particle size (1–0.6 mm) as constant. In the first set, variations in the contact time from 0–180 min were studied, at 0.3 g/100 mL GCG dosage, 7 as the initial pH of solution, and 150 rpm agitation speed. In the second set, the variations were studied at different agitation speeds (0, 50, 100, 150, 200, and 250 rpm), maintaining the contact time at optimum (based on the findings of the first set), with all the other parameters being maintained identical to the first set. In the third set, variations in the initial pH of solution (3–10) were investigated with the contact time kept at the optimum and agitation speed (according to the first and second set findings), maintaining the GCG dosage identical to the first set. Finally, in the last set, variations were studied in the GCG dosage (0.2–2.4 g/mL) with contact time at optimum, and the initial value of pH solution and speed of agitation drawn from the outcomes of the first, second, and third sets, respectively. In the experiments described above, 250 mL plastic Erlenmeyer flasks were used, each of which contained 100 mL of the F⁻ solution with a specified quantity of the GCG dose.

The flasks were then placed in a shaker (Edmund Bühler SM 25, Germany). After accurate and predetermined time intervals, the samples were filtered, and analyses of the filtrates were done to ascertain the fluoride quantity remaining in the solution. The pH variations at the different values were noted by adding either 1 M HCl or 1 M NaOH. The F⁻ removed, in percentage (*R* %) and the quantity of sorbed fluoride (mg/g) retained in the GCG were determined, as shown in Eqs. (1) and (2), respectively [25]:

$$R\% = \frac{C_0 - C_e}{C_0} \times 100 \tag{1}$$

$$q_e = \frac{V(C_0 - C_e)}{m} \tag{2}$$

where C_e and C_0 represent the equilibrium and primary concentrations (mg/L) of the F⁻, respectively. m is the mass of the GCG (g), and V is the volume of the solution (L).

2.6. Sorption isotherm models

The sorption data were described using two isotherm models, as illustrated below [26]:

- *Langmuir model*: this model can be represented using the following equation:

$$q_e = \frac{q_m b C_e}{1 + b C_e} \tag{3}$$

where b is the constant of the free energy of sorption (L/mg), q_m represents the maximum sorption capacity (mg/g), and C_e (mg/L) is the equilibrium F⁻ concentration in the bulk solution.

- *Freundlich model*: this model is quantified by applying the equation given below.

$$q_e = K_F C_e^{1/n} \tag{4}$$

where n is an empirical coefficient indicative of the sorption intensity, and K_F is the Freundlich sorption coefficient.

2.7. Distilled water leaching of fluoride-bearing GCG

Distilled water leaching is ranked among the most significant of the investigative tests used to assess a reactive material in terms of its potential to retain contaminants over a long time period and prohibiting its transformation from the bounded (solid phase) to the soluble (liquid phase). Hence, the F⁻-bearing GCG specimens thus recovered were then leached with distilled water, according to the ASTM D-3987 [27]. Analyses were done of the leachates for the relevant fluoride.

2.8. Column experiments

In order to test the reactivity of the new reactive material in column experiments, simulating the actual PRB operation were conducted in one-dimension. Fig. 1 shows the conceptual plotting for the experimental setup employed
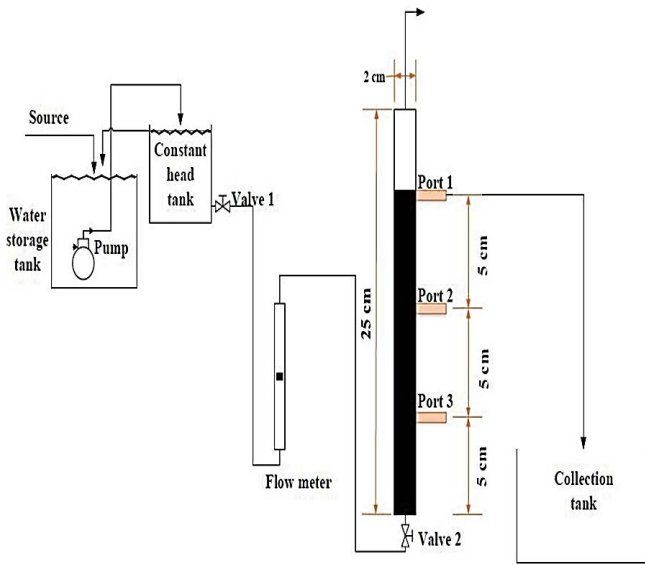
Fig. 1. Schematic diagram of the laboratory-scale column.

in this study, to accomplish the continuous experiments. In this setup, a perspex cylinder 2 cm in diameter and 25 cm in height, valves, flow meter, storage tanks to ensure constant head flow, a flow meter, and a tank for collecting treated water were employed. In the used column, there are three sequentially ports that were located from bottom upwards of the column as follows Port 1 (5 cm), Port 2 (10 cm), and Port 3 (15 cm). In fact, from Fig. 1 it is evident that the column was packed with the GCG. First, distilled water was added gradually to ensure that the GCG medium was saturated. First, the distilled water was introduced slowly at the bottom of the column and forced upward through the column to make sure that all the trapped air among the particles of reactive media (GCG) was expelled and achieve the saturation state. To determine the seepage, three values of flow rate (5, 10, and 15 mL/min) were selected with their respective velocities (3.55, 7.10, and 10.65 cm/min). These values were chosen to fulfill the laminar flow state with Reynolds number (Re) < 1–10 [28]. The fluoride concentrations in the effluent were monitored along the entire column length from the sampling ports for 50 h.

2.9. Fluoride transport and breakthrough curves

Several processes such as sorption, advection, diffusion, precipitation, dispersion, and decay were found to influence the movement of the contaminants in the groundwater system, [19]. The mathematical representation of pollutants movement in a porous media can be shown as the simultaneous solution of the advection–dispersion equation that explains the interactions between the contaminant (F⁻) and medium matrix (GCG). The one-dimensional advection–dispersion equation is shown through the following equation, as cited by Faisal and Abd Ali [29]:

$$n\frac{\partial C}{\partial t} = nD_z\frac{\partial^2 C}{\partial z^2} - nV_z\frac{\partial C}{\partial z} - \rho_b\frac{\partial(q)}{\partial t} \qquad (5)$$

where n is the effective porosity of the porous medium, V_z is the pore water velocity, q is the contaminant mass sorbed on the medium matrix, and nV_z represents the water flow velocity according to Darcy's Law. Thus, the relationship presumed between q and C, is as shown below:

$$q = f(C) \qquad (6)$$

Considering Eq. (5), the transport equation is explained as given below:

$$\frac{\partial C}{\partial t} = \left(\frac{D_z}{R}\right)\frac{\partial^2 C}{\partial z^2} - \left(\frac{V_z}{R}\right)\frac{\partial C}{\partial z} \qquad (7)$$

where R is the retardation factor, represented as follows:

$$R = 1 + \frac{\rho b}{n}\frac{\partial q}{\partial C} \qquad (8)$$

There are two ways to solve Eq. (7), either analytically or numerically. To get the flow domain, the C values calculated are spatially and temporally plotted. These plotted curves are crucial to designing the PRB and predicting the longevity on the field scale [30]. The curve indicated the concentration of the pollutant as a function of time for a specified site on the flow domain (breakthrough curve). It takes an S-shape at the point of continuous and constant influent concentration [31]. As the empirical breakthrough curve models are more simple and manageable than the numerical solution, therefore, they were used for modeling the breakthrough curves in the GCG-column, as explained below:

• Bohart–Adams model [32]

The Bohart–Adams model described the relationship present in a one-dimension sorption system, between the normalized concentration C/C_0 and time. The model is explained as given:

$$\frac{C}{C_0} = \exp\left(KC_0 t - KN_0\frac{Z}{U}\right) \qquad (9)$$

where N_0 is the concentration at the saturation level (mg/L), K is the kinetic constant (L/g/min), U is the flow velocity (cm/min), Z is the bed height (cm), and t is the operation time (min). Also, C_0 and C, respectively, the initial and instantaneous contaminant concentrations in the solution (mg/L).

• Thomas–Bed Depth Service Time (BDST) model [33]

This popular model is used to explain the manner a non-conservative pollutant is transported in a packed column, as shown below:

$$\frac{C}{C_0} = \frac{1}{1 + \exp\left[\frac{K_T}{Q}qM - K_T C_0 t\right]} \qquad (10)$$

where C_0 is the concentration of the influent and C is the concentration of the effluent (mg/L), Q represents the flow

rate (mL/min), q indicates the maximum sorption capacity (mg/g), K_T refers to the Thomas rate constant (mL/mg min), and M is the mass of the reactive material (g).

- Clark model [34]

Clark assumed that contaminant adsorption is subjected to the Freundlich model and hence developed the following kinetic formula:

$$\left(\frac{C}{C_0}\right)^{N-1} = \frac{1}{1 + Ae^{-rt}} \tag{11}$$

where N indicates the exponent of the Freundlich isotherm, while A and r represent the parameters of the kinetic equation.

3. Results and discussion

3.1. Characterization of GCG

3.1.1. FTIR analysis

The FTIR spectra of the glass granules and date juice mixture were noted, pre- and post-burning, as indicated in Fig. 2. However, Table 1 lists the contributions of every single functional group. In Fig. 2a strong peaks are seen in the vicinity of 930, 1,030 and 1,130 cm⁻¹ possibly caused by the sucrose units that exist in the juice of date. At 1,339; 2,725; 2,932 and 3,440 cm⁻¹ the adsorption bands visible indicate the available functional chemical groups of the sucrose present in the date juice. At 465 cm⁻¹ the sharp peak seen is caused by the SiO_2 group of the glass [35]. In Fig. 2b the characteristic graphene peaks visible at 1,596; 1,650; 1,755 and 3,570 cm⁻¹, which clearly demonstrates that the hardened date juice has undergone graphitization [36].

3.1.2. SEM and EDX analysis

The SEM images enabled the study of the morphology of the waste glass granules and the GCG, as indicated in Fig. 3. The GCG revealed the honeycomb-like graphenic

morphology because of the hybridization of the glass surface with an interconnected network of multilayered graphene sheets [37]. Apart from the layered structure, the very rough and wrinkled surface, largely composed of macropores, enabled this highly active surface to be maintained. In theory, these features are assumed to play a crucial role in making the active sites available for the sorption process [38]. Apart from employing the EDX analyzer, primary elements were identified. This showed that the surface of GCG principally consisted of C (70.2%) and O (20.5%), and only traces of silicon, aluminum, sodium, magnesium, and calcium were observed, as listed in Table 2.

3.1.3. Surface area

The specific surface areas of the GCG, before and after activation with a strong acid (H_2SO_4) were assessed as 84 and 168 m²/g, respectively. It must be noted that despite the GCG surface area being less than that of the pristine graphene sheets (which have a high theoretical surface area), it is still capable of fluoride removal. This irregularity is probably due to the graphene sheets present on the

Table 2
Percent weight of elements on the surface of glass waste granules and GCG (EDX analysis)

Element	Weight (%)	
	Glass	GCG
C	–	70.2
O	23.2	20.5
Al	0.4	0.6
Si	62	3.5
S	0.1	0.2
Ca	4	0.9
Na	8	1.3
Mg	2	1
K	0.1	0.3
Fe	0.2	0.5
Total	100	100

Table 1
Functional groups of glass granules and date juice mixture, before and after the burning

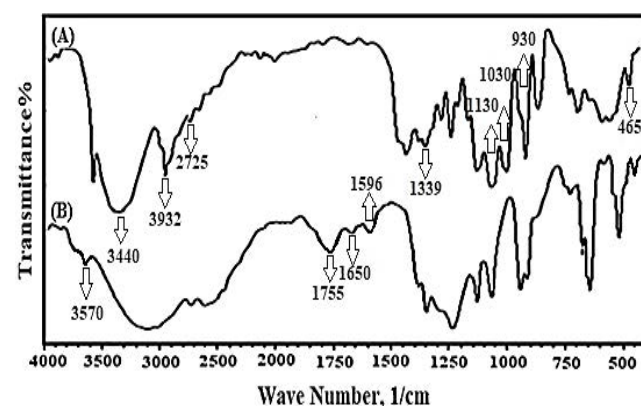| Before burning		After burning	
Wave no. (cm⁻¹)	Type of bond	Wave no. (cm⁻¹)	Type of bond
3,440	O–H	3,570	O–H
2,932	C–H	1,755	C–O
2,725	C–H–O	1,650	C=C
1,339	C–O	1,596	C–C
1,130	C–O–C		
1,030	C–OH		
930	C–H		
465	SiO_2		

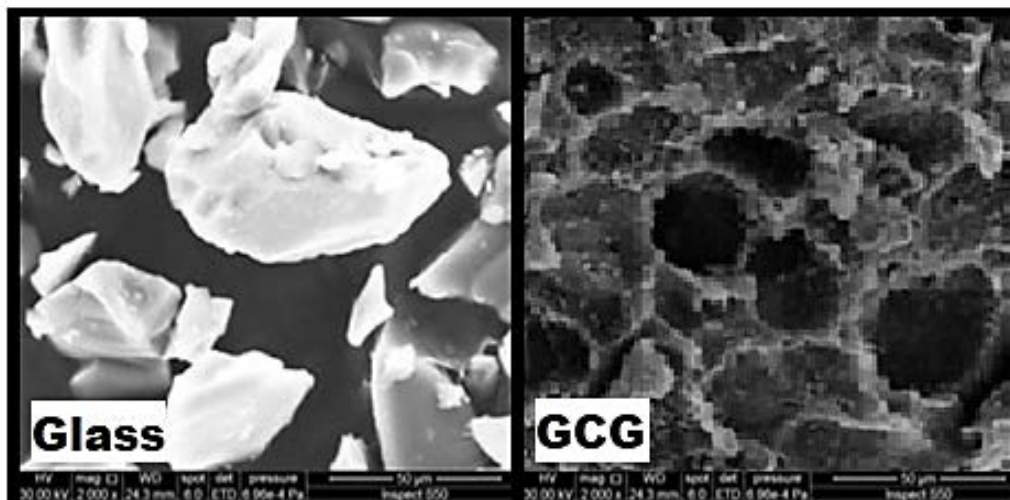Fig. 2. FTIR spectra of glass granules and date's juice mixture (a) before and (b) after burning.

Fig. 3. SEM images of glass waste granules and GCG.

glass surfaces, which offer many active sites at which the sorption can occur, thus facilitating a high degree of fluoride removal [22]. This result corresponds to the findings of Yang et al. [39] in which the specific surface area of the pristine graphene sheets was extensively decreased when coated onto the silica particles.

3.2. Influence of batch-operating parameters

In this study, the optimum conditions required for the maximum removal of fluoride using GCG as the reactive material, were examined by investigating the influence exerted by the contact time, agitation speed, initial pH of solution, and GCG dosage as the principal parameters.

3.2.1. Effect of contact time

Equilibration times in the 0–180 min range were performed as sets of batch experiments, to determine the time needed to reach equilibrium state. From the findings it appeared that the course of F$^-$ removal by GCG was a very quick one. The profile of fluoride removal was observed to involve two sections: rapid rate of F$^-$ removal within 60 min, followed by a slow rate of fluoride removal, until equilibrium as a whole was accomplished after 90 min ($R\% = 35$) as shown in Fig. 4a. The influence exerted by contact time on the GCG-governed removal of fluoride was assessed by employing the initial fluoride concentration of 10 mg F$^-$/L, agitation speed of 150 rpm, pH 7, and GCG of 0.3 g/100 mL.

3.2.2. Effect of agitation speed

From Fig. 4b it is clear that about 10% of the F$^-$ had been removed prior to the shaking process (at 0 agitation). The contact time was determined to be around 90 min, while the rest of the parameters were retained identical to the earlier step. A gradual escalation in the F$^-$ removal capacity was observed as the speed was increased from 0 to 250 rpm (at which nearly 42% of the F$^-$ was removed). This, most likely, was due to the enhanced degree of

F$^-$ diffusing onto the surface of GCG, and thereby, to the greater degree of contact between the binding sites and the F$^-$ [40].

3.2.3. Effect of pH

One of the imperative and highly important parameters, is the pH of the solution because it affects the F$^-$ sorption at the solid–liquid interfaces. The manner that pH influenced the F$^-$ species to attach onto the GCG surface was examined, using a set of experiments that employed 10 mg F$^-$/L as the initial fluoride concentration, with the pH maintained at values from 3 to 10, as depicted in Fig. 4c. The results verified that there was a slight rise in the fluoride uptake as the pH was correspondingly boosted up to 6 ($R\% = 45$). Then, when the pH values exceeded 6, the efficiency of the F$^-$ removal dropped. This decrease was likely because at the higher pH levels, the surface sites of the sorbent would take up more negative charges characterized by the OH$^-$ ions, which would specifically repel the negatively charged F$^-$ available in the solution.

3.2.4. Effect of GCG dosage

Sorbent dosage ranks high among the crucial factors that affect sorption equilibrium. As stated earlier, in this study, under Section 2.5, several GCG doses were applied to establish the optimum dosage for the highest quantity of F$^-$ removal. From the results it is apparent that 2 g of GCG was the optimum value for the highest F$^-$ removal efficiency, which was almost 95%, at pH 6, 250 rpm, and contact time of 90 min, as depicted in Fig. 4d. The increased GCG dose would induce a rise in the fluoride uptake capacity, which was likely because more sorbent surfaces or more numbers of active sites were available for the fluoride uptake to occur. These results concurred with the tendency of the F$^-$ uptake by natural clay, as Ramdani et al. reported [41]. However, when the adsorbent dose was raised to exceed 2 g/100 mL, no corresponding increase in the fluoride removal efficiency was observed. This observation was possibly because of the resistance to the mass
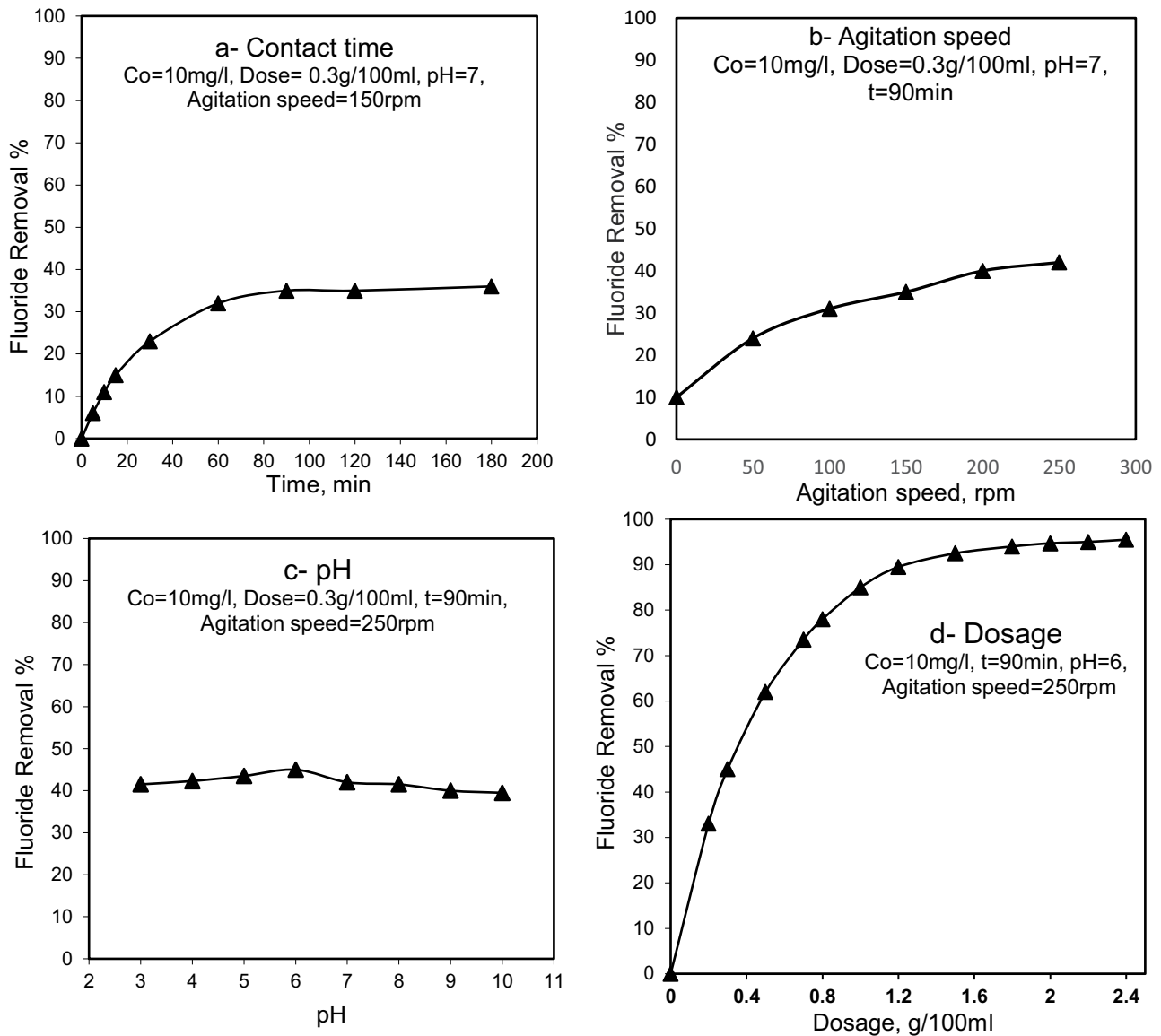
Fig. 4. Profile of fluoride removal percent at different (a) contact time, (b) agitation speed, (c) pH, and (d) GCG dosage.

transport of the F⁻ from the major part of the solution onto the sorbent (GCG) surfaces. This may be the likely explanation for the reason that once the equilibrium or saturation level is reached, the uptake F⁻ percent will be achieved with only a constant pattern, and no increase. This is similar to the concept that increasing the GCG surface will result in an accumulation of the F⁻, resulting in a paucity of effective sites for sorption [42,43].

3.3. Isotherm models

The Langmuir and Freundlich isotherm models were used to fit the experimental sorption data. As shown in Table 3, the parameters of these models were assessed, utilizing the linear form. It is evident that the coefficient of determination (R^2) value was higher for the Freundlich model ($R^2 = 0.9907$) than for the Langmuir model ($R^2 = 0.9640$),

implying that the Freundlich isotherm model was more applicable, as shown in Fig. 5.

3.4. Distilled water leaching of fluoride

The distilled water leaching test was used to study the leaching of fluoride from the GCG granules loaded with fluoride. From the findings it became clear that only a small amount of fluoride was readily soluble. The F⁻ leached was estimated as a percentage of the total F⁻ that had been loaded onto the GCG granules (0.002%). Besides, the leaching test performed for the elements included in the GCG constituents, like Na, Mg, Ca, K, and Fe, as proven by the DX test which revealed that the percentages of the dissolution of these elements usually dropped to below the detection limits, under the conditions of the present experiment. Through this examination, the GCG was confirmed to be
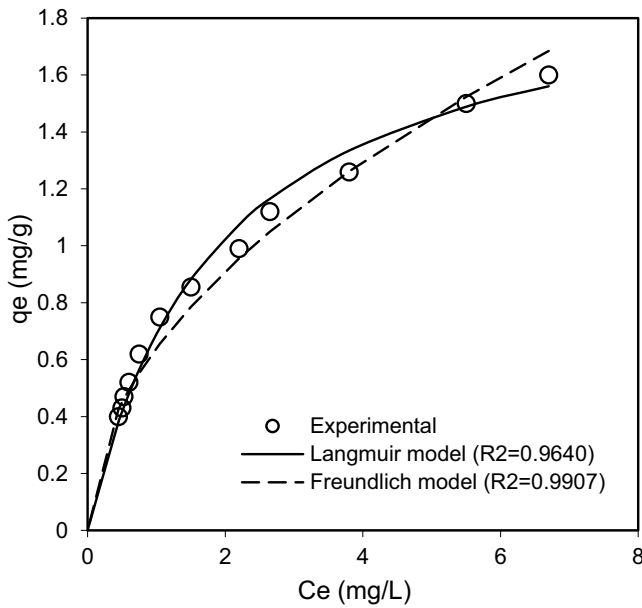
Fig. 5. Plots of the sorption isotherm models and experimental data.

Table 3
Estimated parameters for sorption isotherm models

Isotherm model	Freundlich			Langmuir		
Estimated parameters	K_F	n	R^2	q_m (mg/g)	b (L/mg)	R^2
	0.639	1.962	0.9907	2.006	0.523	0.9640

capable of retaining fluoride, therefore, it can be employed effectively as a reactive material in PRB technology.

3.5. Column tests

A set of column tests was done using a Perspex column having 3 ports, as shown schematically in Fig. 1. These experiments were done utilizing a fluoride solution, applying the best conditions obtained from the batch tests. However, the results achieved from the column experiments are discussed using the indicators listed.

3.5.1. Effect of bed height (thickness of barrier)

In the effluents, the normalized concentration (breakthrough) curves of the fluoride were assessed from the three ports for a 50 h time period, at 10 mg/L of initial F⁻ concentration and 5 mL/min of flow rate, as displayed in Fig. 6a. The F⁻ propagation is clearly seen to be impeded by the GCG-barrier, as well as by the increased thickness of the GCG-barrier (ports P1 of 5 cm, P2 of 10 cm, and P3 of 15 cm) which caused the improvement in the treatment; this is the case, as a thicker barrier suggests that the pollutant is retained for a longer time period within the PRB and the availability of a greater number of sites for sorption to
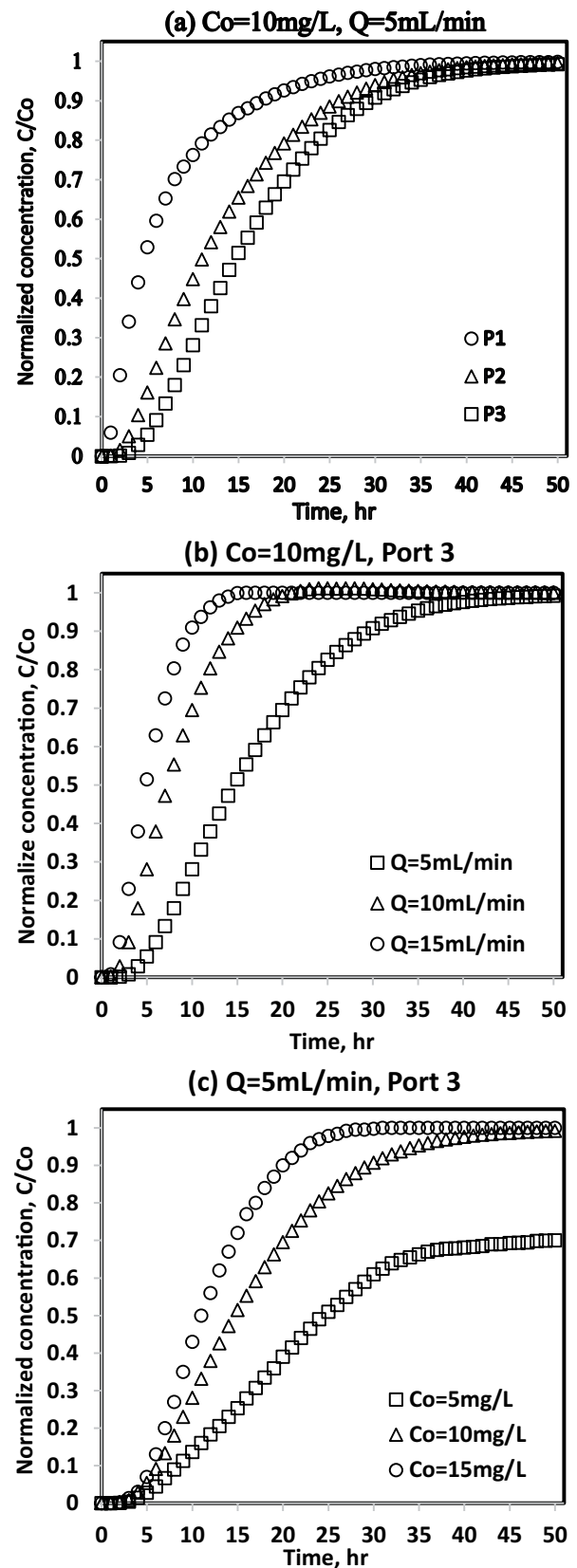

Fig. 6. Normalized concentration (breakthrough) curves of fluoride at different (a) bed height, (b) flow rates, and (c) and initial F⁻ concentration.

occur. However, as the time increases the barrier begins to achieve saturation, which thus lessens the effect of the factor of fluoride retardation, implying a lowering in the functionality percent of the GCG-barrier.

3.5.2. Effect of flow rate

In Fig. 6b the normalized concentration (breakthrough) curves obtained during different values of flow rates (5, 10 and 15 mL/min), constant bed height (P3, 15 cm), and initial F$^-$ concentration (10 mg/L), are shown. This figure reveals that when the value of flow rate increases, it will promote the velocity of flow which, in turn, will boost the propagation of the contaminant front. It is also clear that the barrier functionality will get reduced as the flow rate and contact time increase. This is because the increasing quantity of the fluoride that penetrates the barrier causes a reduction in the GCG-barrier functionality in retarding the fluoride. However, at the high flow rate, it was clear that resident time of the F$^-$ was lowered and hence the F$^-$ were in contact with the sorbent (GCG) for shorter time periods. This result concurred with the findings of some researchers such as Mohan et al. [44]. Thus, it is evident that at a lower flow rate, the column efficiency is at its maximum.

3.5.3. Effect of initial fluoride concentration

In Fig. 6c the influence exerted by the initial F$^-$ concentrations of 5, 10, 15 mg/L on the fluoride sorption using the GCG-barrier is shown, for 5 mL/min flow rate and P3, 15 cm bed depth. The lower influent F$^-$ concentration is observed to produce higher treatment efficiency. This is likely because the lower concentration means that fewer available active sites are required for the sorption to occur, and therefore, the reactive material takes much longer time to get exhausted or saturated ($C/C_0 = 1$), thus improving the sorption process. However, it appears that the bed starts to get saturated as the travel time and initial concentration increases; this confirms a decrease in the F$^-$ retardation factor, thus implying a reduction in the GCG functionality (in percentage).

3.5.4. Breakthrough curve models

The findings regarding the influence exerted by the experiments with bed height (Section 3.5.1) were fitted to the Bohart–Adams, Thomas–BDST, and Clark models, as indicated in Fig. 7. The breakthrough curves of fluoride

at all three ports (1, 2, and 3) were represented by these empirical models by applying the nonlinear regression analysis method in version 2007 of Microsoft Excel. In Table 4, the values of the model's constants and determination coefficient (R^2) are shown for the experimental and predicted results of the current column experiments. For all three models, it was mandatory to comprehend the manner in which the rate of the contaminant front was transported along the entire length of the barrier tested, and at all the curves. In this regard, it is evident that it is critical, during the design process, to use the breakthrough point. Therefore, employing the apt model to represent the experimental tests appears to be the best way to determine this point. Therefore, by using the coefficient of determination (R^2), the degree of concurrence seen between the experimental values and predicted ones can be specified. Thus, from all the results and analyses, the Clark model is believed to best represent the ones tested, as shown in Table 4.

4. Conclusion

- As low-grade Iraqi date juice and granules of glass waste were used, it facilitated the green synthesis of the novel, economic, and effective reactive media, which involved glass granules coated with graphene sheets, called GCG.
- From the batch results it was evident that the parameters of contact time, agitation speed, pH, and GCG dosage strongly affected the fluoride sorption process, with 10 mg/L as the initial F$^-$ concentration and 1–0.6 mm as particle size. For these parameters, the best values of were found to be 90 min, 250 rpm, 6 and GCG of 2 g/100 mL, respectively, which guaranteed removal efficiency at a maximum of around 95%.
- From the experimental findings it is clear that the data of sorption can be represented by the Freundlich isotherm model, with 0.9907 determination coefficient.
- While the FTIR spectra confirmed the graphene deposited on the glass surface, the SEM/EDX revealed that the GCG surface had the characteristic heterogeneous and porous features believed to be one of the main reasons that facilitated the effective fluoride removal.
- The models of breakthrough curve, namely, the Bohart–Adams, Thomas–BDST, and Clark models were fitted with the continuous experimental results. The Clark model found better than two other models on breakthrough curves description throughout the length of the

Table 4
Parameters of breakthrough models with determination coefficients corresponding to the experimental conditions

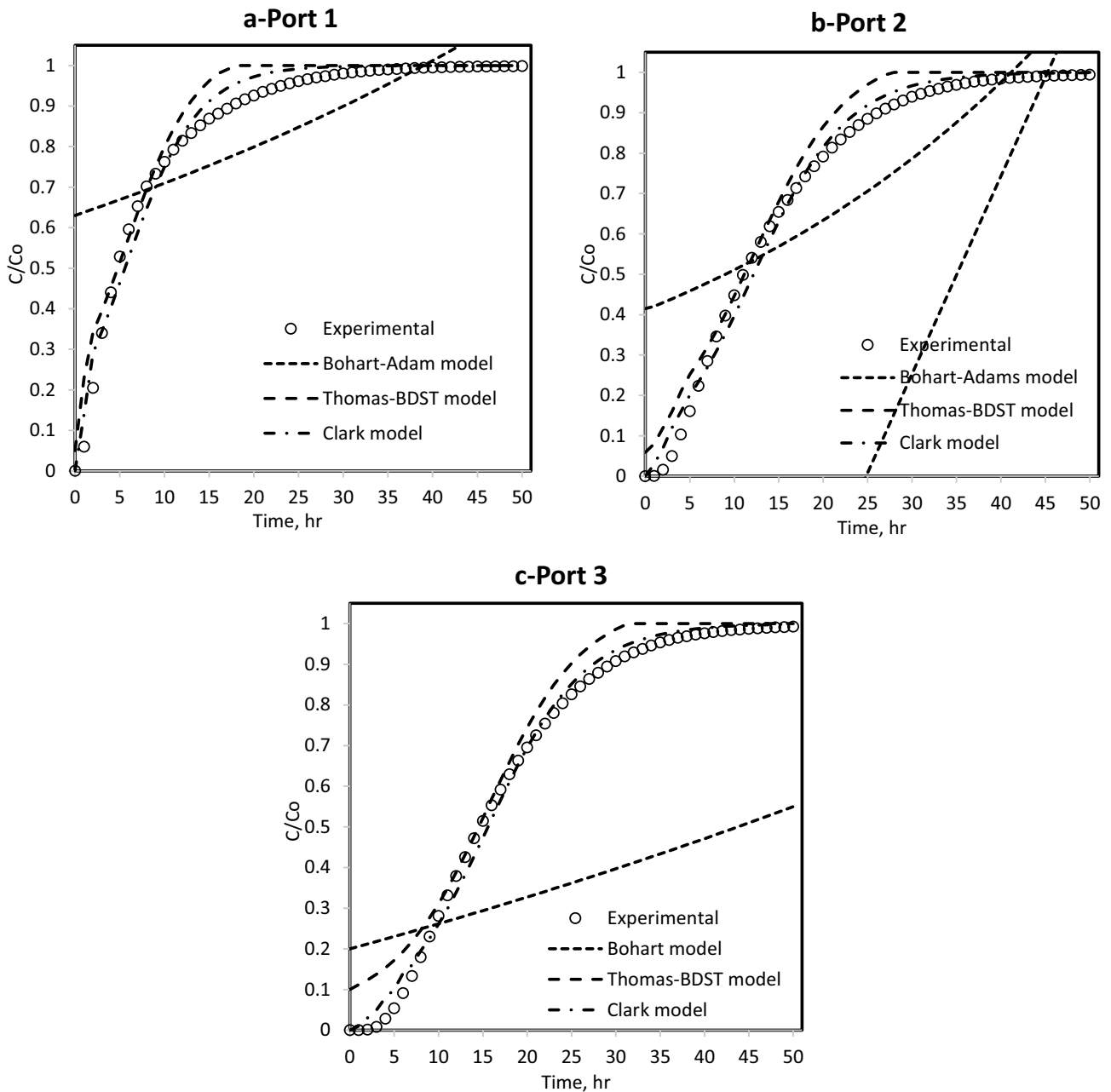| Ports	Breakthrough models								
	Bohart–Adams			Thomas–BDST			Clark		
	KC_0	KN_0Z/U	R^2	K_TC_0	K_TqM/Q	R^2	A	r	R^2
P1	0.1971	460.8796	0.6504	4.1354	1.3842	0.9850	3.7431	0.0041	0.9901
P2	0.3594	887.3615	0.7189	3.1786	2.3275	0.9799	9.4686	0.0031	0.9949
P3	0.1000	0.1000	0.4811	3.1047	2.9048	0.9701	16.7024	0.0030	0.9965

a-Port 1

b-Port 2

c-Port 3

Fig. 7. Variation of fluoride normalized concentration sorbed onto GCG as a function of time for (a) P1, (b) P2, and (c) P3.

barrier adopted, having a coefficient of determination in the 0.9901 to 0.9965 range, in all the experiments.

• Finally, from the batch and continuous investigations, the GCG appeared to be efficient as a sorbent and was found to be a successful reactive medium in the PRB, able to remediate the fluoride-contaminated groundwater, with credible removal efficiency, under the conditions of the present experimental work.

References

[1] A.A. Mohammed, Z.T. Abd Ali, Z.B. Masood, A comparative isothermal and kinetic study of the removal of lead(II) from aqueous solution using different sorbents, Assoc. Arab Univ. J. Eng. Sc., 25 (2018) 1–21.

[2] Z.B. Masood, Z.T. Abd Ali, Numerical modeling of two-dimensional simulation of groundwater protection from lead using different sorbents in permeable barriers, Environ. Eng. Res., 25 (2020) 605–613.

[3] X.X. Wang, X. Li, J.Q. Wang, H.T. Zhu, Recent advances in carbon nitride-based nanomaterials for the removal of heavy

metal ions from aqueous solution, J. Inorg. Mater., 35 (2020) 260–270.

[4] X.L. Liu, H.W. Pang, X.W. Liu, Q. Li, N. Zhang, L. Mao, M.Q. Qiu, B.W. Hu, H. Yang, X.K. Wang, Orderly porous covalent organic frameworks-based materials: superior adsorbents for pollutants removal from aqueous solutions, Innovation, 2 (2021) 100076, doi: 10.1016/j.xinn.2021.100076.

[5] Q.Q. Cai, B.D. Turner, D.C. Sheng, S. Sloan, Application of kinetic models to the design of a calcite permeable reactive barrier (PRB) for fluoride remediation, Water Res., 130 (2018) 300–311.

[6] S. Chatterjee, M. Mukherjee, S. De, Groundwater defluoridation and disinfection using carbonized bone meal impregnated polysulfone mixed matrix hollow-fiber membranes, J. Water Process Eng., 33 (2020) 101002, doi: 10.1016/j.jwpe.2019.101002.

[7] E.M. Nigri, M.A.P. Cechinel, D.A. Mayer, L.P. Mazur, J.M. Loureiro, S.D.F. Rocha, V.J.P. Vilar, Cow bones char as a green sorbent for fluorides removal from aqueous solutions: batch and fixed-bed studies, Environ. Sci. Pollut. Res., 24 (2017) 2364–2380.

[8] M. Talat, S. Mohan, V. Dixit, D.K. Singh, S.H. Hasan, O.N. Srivastava, Effective removal of fluoride from water by coconut husk activated carbon in fixed bed column: experimental and breakthrough curves analysis, Groundwater Sustainable Dev., 7 (2018) 48–55.

[9] S. Srivastava, S.J.S. Flora, Fluoride in drinking water and skeletal fluorosis: a review of the global impact, Curr. Environ. Health Rep., 7 (2020) 140–146.

[10] A. Singh, A.K. Patel, M. Kumar, Mitigating the Risk of Arsenic and Fluoride Contamination of Groundwater Through a Multi-Model Framework of Statistical Assessment and Natural Remediation Techniques, M. Kumar, D. Snow, R. Honda, Eds., Emerging Issues in the Water Environment during Anthropocene, Springer, Singapore, 2020, pp. 285–300.

[11] AA.H. Faisal, Z.T. Abd Ali, Remediation of groundwater contaminated with the lead–phenol binary system by granular dead anaerobic sludge-permeable reactive barrier, Environ. Technol., 38 (2017) 2534–2542.

[12] Z.T. Abd Ali, H.M. Flayeh, M.A. Ibrahim, Numerical modeling of performance of olive seeds as permeable reactive barrier for containment of copper from contaminated groundwater, Desal. Water Treat., 139 (2019) 268–276.

[13] A.A.H. Faisal, Z.T. Abd Ali, Using sewage sludge as a permeable reactive barrier for remediation of groundwater contaminated with lead and phenol, Sep. Sci. Technol., 52 (2017) 732–742.

[14] Z.T. Abd Ali, Green synthesis of graphene-coated sand (GCS) using low-grade dates for evaluation and modeling of the pH-dependent permeable barrier for remediation of groundwater contaminated with copper, Sep. Sci. Technol., 56 (2021) 14–25.

[15] U. Kumarasinghe, K. Kawamoto, T. Saito, Y. Sakamoto, M.I.M. Mowjood, Evaluation of applicability of filling materials in permeable reactive barrier (PRB) system to remediate groundwater contaminated with Cd and Pb at open solid waste dump sites, Process Saf. Environ. Prot., 120 (2018) 118–127.

[16] A.H. Sulaymon, A.A.H. Faisal, Z.T. Abd Ali, Performance of granular dead anaerobic sludge as permeable reactive barrier for containment of lead from contaminated groundwater, Desal. Water Treat., 56 (2015) 327–337.

[17] A.A.H. Faisal, Z.T. Abd Ali, Groundwater protection from lead contamination using granular dead anaerobic sludge biosorbent as permeable reactive barrier, Desal. Water Treat., 57 (2016) 3891–3903.

[18] Z.T. Abd Ali, Using activated carbon developed from Iraqi date palm seeds as permeable reactive barrier for remediation of groundwater contaminated with copper, Al-Khwarizmi Eng. J., 12 (2016) 34–44.

[19] A.A. Faisal, Z.T. Abd Ali, Phenol removal using granular dead anaerobic sludge permeable reactive barrier in a simulated groundwater pilot plant, J. Eng., 20 (2014) 63–79.

[20] A.F. Ali, Z.T. Abd Ali, Sustainable use of concrete demolition waste as reactive material in permeable barrier for remediation

of groundwater: batch and continuous study, J. Environ. Eng., 146 (2020) 04020048.

[21] S. Sen Gupta, T.S. Sreeprasad, S.M. Maliyekkal, S.K. Das, T. Pradeep, Graphene from sugar and its application in water purification, ACS Appl. Mater. Interfaces, 4 (2012) 4156–4163.

[22] R. Dubey, J. Bajpai, A.K. Bajpai, Green synthesis of graphene sand composite (GSC) as novel adsorbent for efficient removal of Cr(VI) ions from aqueous solution, J. Water Process Eng., 5 (2015) 83–94.

[23] R. Rezaee, S. Nasseri, A.H. Mahvi, R. Nabizadeh, S.A. Mousavi, A. Maleki, M. Alimohammadi, A. Jafari, S.H. Borji, Development of a novel graphene oxide-blended polysulfone mixed matrix membrane with improved hydrophilicity and evaluation of nitrate removal from aqueous solutions, Chem. Eng. Commun., 206 (2019) 495–508.

[24] E. Ruiz-Hitzky, M. Darder, F.M. Fernandes, E. Zatile, F.J. Palomares, P. Aranda, Supported graphene from natural resources: easy preparation and applications, Adv. Mater., 23 (2011) 5250–5255.

[25] J. Wang, C. Chen, Biosorbents for heavy metals removal and their future, Biotechnol. Adv., 27 (2009) 195–226.

[26] N. Saad, Z.T. Abd Ali, L.A. Naji, A.A.A.H. Faisal, N. Al-Ansari, N. Saad, Z.T. Abd Ali, L.A. Naji, A.A.A.H. Faisal, N. Al-Ansari, Development of Bi-Langmuir model on the sorption of cadmium onto waste foundry sand: effects of initial pH and temperature, Environ. Eng. Res., 25 (2019) 677–684.

[27] H. Yılmaz, Characterization and comparison of leaching behaviors of fly ash samples from three different power plants in Turkey, Fuel Process. Technol., 137 (2015) 240–249.

[28] J.H. Cushman, D.M. Tartakovsky, Eds., The Handbook of Groundwater Engineering, CRC Press, Boca Raton, 2016.

[29] A.A.H. Faisal, Z.T. Abd Ali, Using granular dead anaerobic sludge as permeable reactive barrier for remediation of groundwater contaminated with phenol, J. Environ. Eng., 141 (2015) 04014072.

[30] Z.T. Abd Ali, Combination of the artificial neural network and advection-dispersion equation for modeling of methylene blue dye removal from aqueous solution using olive stones as reactive bed, Desal. Water Treat., 179 (2020) 302–311.

[31] G. Shaverdi, Developing a Model for Mass Transfer in Adsorption Packed-Bed Filters, Degree of Master of Applied Science (Mechanical Engineering) at Concordia University, Montreal, Quebec, Canada, 2012.

[32] G.S. Bohart, E.Q. Adams, Some aspects of the behavior of charcoal with respect to chlorine, J. Am. Chem. Soc., 42 (1920) 523–544.

[33] H.C. Thomas, Heterogeneous ion exchange in a flowing system, J. Am. Chem. Soc., 66 (1944) 1664–1666.

[34] R.M. Clark, Evaluating the cost and performance of field-scale granular activated carbon systems, Environ. Sci. Technol., 21 (1987) 573–580.

[35] J.C. Tewari, K. Malik, In situ laboratory analysis of sucrose in sugarcane bagasse using attenuated total reflectance spectroscopy and chemometrics, Int. J. Food Sci. Technol., 42 (2007) 200–207.

[36] C. Shan, H. Yang, D. Han, Q. Zhang, A. Ivaska, L. Niu, Water-soluble graphene covalently functionalized by biocompatible poly-L-lysine, Langmuir, 25 (2009) 12030–12033.

[37] Y. Tao, D. Kong, C. Zhang, W. Lv, M. Wang, B. Li, Z.-H. Huang, F. Kang, Q.-H. Yang, Monolithic carbons with spheroidal and hierarchical pores produced by the linkage of functionalized graphene sheets, Carbon, 69 (2014) 169–177.

[38] S. Khan, A.A. Edathil, F. Banat, Sustainable synthesis of graphene-based adsorbent using date syrup, Sci. Rep., 9 (2019) 1–14.

[39] K. Yang, B. Chen, L. Zhu, Graphene-coated materials using silica particles as a framework for highly efficient removal of aromatic pollutants in water, Sci. Rep., 5 (2015) 11641, doi: 10.1038/srep11641.

[40] J. Anwar, U. Shafique, M. Salman, A. Dar, S. Anwar, Removal of Pb(II) and Cd(II) from water by adsorption on peels of banana, Bioresour. Technol., 101 (2010) 1752–1755.

[41] A. Ramdani, S. Taleb, A. Benghalem, N. Ghaffour, Removal of excess fluoride ions from Saharan brackish water by adsorption on natural materials, Desalination, 250 (2010) 408–413.

[42] M. Habuda-Stanić, M. Ergović Ravančić, A. Flanagan, A review on adsorption of fluoride from aqueous solution, Materials, 7 (2014) 6317–6366.

[43] J. Přech, K.N. Bozhilov, J. El Fallah, N. Barrier, V. Valtchev, Fluoride etching opens the structure and strengthens the active sites of the layered ZSM-5 zeolite, Microporous Mesoporous Mater., 280 (2019) 297–305.

[44] S. Mohan, D.K. Singh, V. Kumar, S.H. Hasan, Effective removal of fluoride ions by rGO/ZrO$_2$ nanocomposite from aqueous solution: fixed bed column adsorption modelling and its adsorption mechanism, J. Fluorine Chem., 194 (2017) 40–50.